Spectral Separability of Vegetation Classes in a Dry, Tropical Region of India Using IRS-1A LISS-1 Data

by

C.S. Jha[1], A.K. Tiwari[2] and J.S. Singh[3]

ABSTRACT

This paper describes the spectral separability of IRS-1A LISS-I data for vegetation classification. Separability was assessed for enhanced data (principal component analysis and hue saturation intensity transformation) as well as for raw IRS bands. The analysis indicated that the enhanced data do not show a superior performance in comparison to the 4 bands of IRS data. The comparison of bands 2, 3 and 4 of IRS with the enhanced data showed that the three PCA bands as well as the HSI transformation bands increase the vegetation class separability significantly.

1.0 Introduction

Remote sensing is a useful tool in monitoring and inventorying land use and vegetation (Aldrich 1975, Tateishi *et al.* 1991, Murai and Honda 1991 and Tiwari *et al.* 1991). Information extraction from satellite data can be done through visual interpretation (Beaubien 1986) or through computer-aided digital processing (Horler and Ahren 1986). The identification of various vegetation or land-cover classes from remotely sensed data is mainly dependent on their spectral response and spectral separability (Jenson 1986 and Singh 1987). A number of enhancement algorithms are currently available to increase the spectral separability between classes (Sabins 1987 and Jenson). Most of the studies carried out on vegetation class identification using enhanced data have been based on visual separation of classes. Assessments of the spectral separability of vegetation cover classes have been carried out for northeastern India by Singh using Landsat MSS data, for the western Himalayan forests by Tiwari *et al.* using IRS-1A LISS-I data and for the Andaman Island forests by Roy *et al.* (1991) using Landsat TM data. However, no literature is available on spectral separability of dry tropical vegetation types.

The study described below was aimed at assessing the spectral separability of vegetation classes in a part of the Vindhyan Hills, India using IRS-1A LISS-I data. The impact of multiband image enhancements on spectral separability was also assessed.

2.0 Study Area

The study area lies between 23°50' and 24°40'N latitude and between 82°25' and 83°32'E longitude in the Vindhyan Hills of Uttar Pradesh, India. The area has a seasonally dry tropical climate, dominated by a typical monsoon season. There are three seasons: winter (November to February), summer (April to June) and rainy (July to September). March and October are transition months between winter and summer and between the rainy season and winter, respectively. The temperature ranges from 10° to 25°C in winter and from 30° to 45°C in summer. The average annual rainfall is 820 mm, of which 86 per cent is contributed by the monsoon.

3.0 Method

A subscene of 1,300 x 1,300 pixels was extracted from an IRS-1A LISS-I scene of 16 October 1988. Digital processing was carried out using a VAX 11/780 computer with VIPS-32 and indigenous software at the Regional Remote Sensing Service Centre, Dehra Dun. Two kinds of multiband image enhancements were carried out for the study: principal component analysis (PCA) and hue saturation intensity transformation (HSI).

[1] National Remote Sensing Agency, Hyderabad, India.

[2] Regional Remote Sensing Service Centre, Dehra Dun, India.

[3] Botany Department, Banaras Hindu University, Varanasi, India.

The purpose of PCA is to compress all the information from the original four-band data into fewer principal components. The procedure employs a linear transformation in which the axis of the original variable is geometrically rotated. The output PCA images are then normalized with a Gaussian stretch.

In HSI transformation, hue refers to the dominant or average wavelength of the light contributing to a colour; saturation specifies the purity of the colour relative to grey; and intensity relates to the total brightness of a colour. In the hexagon model approach, intensity is defined by the distance along the grey line from black to any given hexagonal projection. Hue is expressed by the angle around the hexagon, and saturation as the distance from the grey point at the centre of the hexagon. The farther away from the grey point, the more saturated the colour (Schowengerdt 1983). For the HSI transformation, bands 2, 3 and 4 of the IRS-1 LISS-I data were normalized using a Gaussian stretch.

Unsupervised classification was carried out using all four IRS bands to obtain firsthand information on classification possibilities. The classification resulted in 40 classes, which were regrouped after field checking to generate a vegetation map (Figure 1). From this map, nine classes representing relatively pure vegetation classes on the ground were identified. In each of these classes, sample windows of 150 to 200 pixels were identified. There was no mixing of other classes on the ground within these windows. The windows were used to generate a groundtruth mask and to compute spectral statistics using all four IRS bands, three IRS bands (2, 3 and 4), all HSI bands and all PCA bands as input.

The spectral statistics for various classes were used to generate divergence matrices. The divergence matrices were converted to transformed divergence matrices, which scaled the divergence values between 0 and 2,000 (Kumar and Silva 1977). A transformed divergence value of 2,000 was considered to show excellent separability; 1,900 to <2,000, good separability; and 1,700 to <1,900, moderate separability. Transformed divergence values of <1,700 were considered to show poor separation.

4.0 Results and Discussion

4.1 Visual Interpretability of Vegetation Classes

The false colour composite of IRS bands 4, 3 and 2 mainly depicted two forest classes, i.e., closed and open. In the FCC, tree savannas could not be separated from open forests; degraded grass savannas could not be separated from nonforests; and mixed forests, *Shorea*-dominated forests (SDF) and *Acacia*-dominated forests (ADF) could not be separated.

A colour composite generated by passing PCA bands 1, 2 and 3 through red, green and blue planes led to a somewhat better identification of classes. In the PCA colour composite, mixed forest classes with more than 50 per cent crown cover (M1) and with 40 to 50 per cent crown cover (M2) were separated in a few areas. In some cases, tree savanna classes with *Holarrhena* (TSH) and with *Zizyphus* (TSZ) were merged with M2. *Acacia*- and *Shorea*-dominated forests (ADF and SDF, respectively) could not be separated from the mixed forest with 30 to 40 per cent crown cover (M3). These three classes (ADF, SDF and M3) were, however, collectively separated from other classes. Grass savanna (GS) and degraded grass savanna (DGS) could not be identified precisely.

The colour composite generated using HSI transformation images indicated that TSH and M3 can be separated from each other, as well as from other classes. *Shorea*- and *Acacia*-dominated forests could not be separated from each other but were collectively identified as a single class.

4.2 Statistical Analysis of Separability

The spectral response of various vegetation classes in different IRS-1A LISS-I bands is presented in Figure 2. Three classes of mixed forest (M1, M2 and M3) exhibited very close mean digital number (DN) values in bands 1, 2 and 3, but they could be separated from each other in band 4. *Shorea*-dominated forests exhibited wide overlap with mixed forest classes in the first three bands (1, 2 and 3). The two classes of mixed forest (M1 and M2) with greater than 40 per cent crown cover were discriminated in band 4. In the same band, the M3 class marginally overlapped the *Shorea*-dominated forests class. *Acacia*-dominated forests exhibited overlap with SDF as well as with TSH in band 1. ADF was distinguished from TSH in bands 2 and 3 and from SDF in band 4.

The principal component analysis changed the data structure through multidimensional axis rotation. The first principal component represented

72.13 per cent of the information (Table 1) and corresponded with the soil brightness index of the tasselled cap transformation (Kauth and Thomas 1976). The highest mean DN value in PCA 1 was observed for degraded grass savanna (Figure 3), which included a higher proportion of bare soil areas than did other vegetation types. The lowest mean DN values were recorded for M1 and M2. PCA 2 represented 25.41 per cent of the information and exhibited a trend similar to the tasselled cap greenness index. The general pattern of mean DN values for various classes was similar to that of band 4 of the original IRS data, except for the M3 class, which overlapped with SDF and TSZ in band 4 but was separated in PCA 2. PCA 3 represented only 2.46 per cent of the information. All the classes had high standard deviation values, which indicates a considerable overlapping of classes.

The hue saturation intensity image indicated overlapping digital numbers for all the forest and tree savanna classes (Figure 4). Grass savanna (GS) and degraded grass savanna (DGS) overlapped each other. The lower values for forest and tree savanna classes reflect their position in the red portion of the spectrum in the FCC of raw IRS bands, and the intermediate values for GS and DGS represent the yellow region of the spectrum. Colour saturation was, in general, higher for mixed forests, *Shorea*-dominated forests and tree savanna with *Zizyphus*. The lowest saturation was observed for the GS and DGS classes. The absorption of red light by the photosynthetic parts of the vegetation and the resulting lower DN values in the original IRS band 3 mainly serve to regulate the saturation of vegetation classes. The higher the absorption in the red band (band 3), the higher the saturation. The trend of saturation can thus be considered as an indicator of the productive potential of the vegetation classes. The highest intensity values were recorded for M3, followed by the degraded grass savanna. The lowest intensity was exhibited by M1 and M2.

Pairwise transformed divergence matrices were generated for the raw IRS bands and for the enhanced data. The transformed divergence matrices for all four IRS bands, for three IRS bands (bands 2, 3 and 4), for the HSI transformation and for the PCA are presented in Tables 2, 3, 4 and 5, respectively. The four raw bands of IRS-1A LISS-I exhibited poor separability only for one class pair, i.e., M1 and M2, while the three IRS bands, which are commonly used for the generation of FCCs (bands 2, 3 and 4), showed poor spectral separability between the following classes: M1 and M2, M1 and T52, M2 and T52, M3 and T52, and M3 and SDF. The HSI images generated from IRS bands 2, 3 and 4 exhibited results comparable to those from the four raw IRS bands. However, the class pairs ADF and TSH, and GS and DGS, which represented moderate separability in four IRS bands, were poorly separated in the HSI transformation. Among these two classes, the former had a moderate separability in the three IRS bands (2, 3 and 4). The principal component analysis output bands (3 bands) exhibited a performance similar to that of the HSI transformation. The class pairs DGS and GS, and ADF and TSZ did, however, show better separability in the PCA bands than in the HSI transformation. On the other hand, HSI exhibited a better separability performance for the class pairs M1 and SF, M3 and TSZ, M3 and GS, SF and GS, and AF and GS.

Table 1. Statistics for principal component analysis

	Correlation Matrix			
	Ba1	**Ba2**	**Ba3**	**Ba4**
Ba1	1.000	0.944	0.879	0.317
Ba2	0.944	1.000	0.952	0.103
Ba3	0.879	0.952	1.000	0.023
Ba4	0.317	0.103	−0.023	1.000

	PCA Output Bands					
Output bands	**Coefficients of eigen vectors**				**Eigen values**	**Percentage of information**
	Ba1	**Ba2**	**Ba3**	**Ba4**		
1	0.57484	0.57906	0.56212	0.351390	2.885320	72.133
2	0.10585	−0.12484	−0.21130	0.963619	1.016402	25.410
3	0.62052	0.15151	−0.73997	−0.210790	0.009438	1.859

Table 2. Pairwise class divergence and transformed divergence (in parentheses) for four raw IRS LISS-I bands

Class	M1	M2	M3	SDF	ADF	TSH	TSZ	GS
M2	11.5 (1,525.0)	0.0						
M3	49.0 (1,995.6)	38.9 (1,984.5)	0.0					
SDF	64.1 (1,999.3)	56.9 (1,998.4)	22.9 (1,885.7)	0.0				
ADF	75.2 (1,999.8)	57.0 (1,998.4)	62.6 (1,999.2)	151.1 (2,000.0)	0.0			
TSH	28.4 (1,942.6)	18.2 (1,794.2)	61.7 (1,999.1)	137.3 (2,000.0)	17.0 (1,761.1)	0.0		
TSZ	24.0	47.9	24.1	78.3	58.1	41.1	0.0	
GS	142.9 (2,000.0)	100.0 (2,000.0)	63.7 (1,999.3)	92.1 (2,000.0)	55.9 (1,998.2)	110.7 (2,000.0)	143.7 (2,000.0)	0.0
DGS	270.9 (2,000.0)	223.4 (2,000.0)	129.1 (2,000.0)	140.3 (2,000.0)	178.7 (2,000.0)	276.4 (2,000.0)	251.3 (2,000.0)	17.0 (1,761.1)

Table 3. Pairwise class divergence and transformed divergence (in parentheses) for three raw IRS LISS-I bands (bands 2, 3 and 4)

Class	M1	M2	M3	SDF	ADF	TSH	TSZ	GS
M2	0.3 (73.6)	0.0						
M3	3.3 (1,324.0)	3.3 (1,324.0)	0.0					
SDF	47.6 (1,994.8)	32.3 (1,964.7)	14.5 (1,673.5)	0.0				
ADF	63.7 (1,999.3)	56.9 (1,998.4)	30.9 (1,958.0)	120.0 (2,000.0)	0.0			
TSH	19.7 (1,829.6)	17.3 (1,769.9)	8.4 (1,300.1)	97.6 (2,000.0)	16.5 (1,745.7)	0.0		
TSZ	12.1 (1,559.0)	10.8 (1,481.5)	4.4 (846.1)	73.3 (1,999.8)	20.6 (1,847.7)	1.6 (362.5)	0.0	
GS	121.4 (2,000.0)	93.2 (2,000.0)	51.4 (1,996.8)	46.7 (1,994.2)	53.9 (1,997.6)	105.4 (2,000.0)	99.2 (2,000.0)	0.0
DGS	254.3 (2,000.0)	203.4 (2,000.0)	123.7 (2,000.0)	103.1 (2,000.0)	168.5 (2,000.0)	254.7 (2,000.0)	232.9 (2,000.0)	11.3 (1,512.9)

A study of the transformation divergence matrices suggests that the HSI transformation is best suited for vegetation identification in the study area if only three bands are to be taken as input, especially when HSI is to replace the normal FCC bands. The first three principal components can also replace the normal FCC bands. The selection of HSI or PCA is dependent on the classes that are to be given priority for higher accuracy. Neither HSI nor PCA could provide better separability than when all four raw IRS bands were used.

5.0 Conclusions

The study indicated that the four raw IRS bands produce the best spectral separability for vegetation classification. However, if the number of bands is to be restricted to three, HSI and PCA provide results closer to those from the four IRS bands. However, the performance of HSI and PCA is far better in comparison to the three IRS bands (2, 3 and 4) that are commonly used for the generation of a standard FCC.

Table 4. Pairwise class divergence and transformed divergence (in parentheses) for the first three principal components

Class	M1	M2	M3	SDF	ADF	TSH	TSZ	GS
M2	11.5 (1,525.0)	0.0						
M3	48.8 (1,995.5)	39.9 (1,985.8)	0.0					
SDF	51.4 (1,996.8)	53.1 (1,997.4)	17.4 (1,732.8)	0.0				
ADF	74.5 (1,999.8)	58.2 (1,998.6)	60.4 (1,998.9)	128.1 (2,000.0)	0.0			
TSH	21.1 (1,937.4)	17.1 (1,764.1)	60.8 (1,999.0)	106.5 (2,000.0)	16.7 (1,752.0)	0.0		
TSZ	23.0 (1,889.2)	47.8 (1,994.9)	23.3 (1,891.3)	53.5 (1,997.5)	56.6 (1,998.3)	41.1 (1,988.3)	0.0	
GS	132.5 (2,000.0)	100.1 (2,000.0)	53.4 (1,997.5)	78.6 (1,999.9)	53.1 (1,997.5)	99.6 (2,000.0)	125.3 (2,000.0)	0.0
DGS	248.4 (2,000.0)	219.9 (2,000.0)	108.4 (2,000.0)	118.0 (2,000.0)	170.1 (2,000.0)	268.0 (2,000.0)	212.5 (2,000.0)	53.4 (1,997.5)

Table 5. Pairwise class divergence and transformed divergence (in parentheses) for HSI transformed bands

Class	M1	M2	M3	SDF	ADF	TSH	TSZ	GS
M2	12.5 (1,553.7)	0.0						
M3	46.3 (1,993.9)	37.4 (1,980.4)	0.0					
SDF	105.6 (2,000.0)	46.4 (1,993.9)	26.4 (1,926.2)	0.0				
ADF	64.8 (1,999.4)	48.3 (1,995.2)	45.5 (1,993.2)	123.2 (2,000.0)	0.0			
TSH	26.4 (1,926.2)	16.0 (1,729.3)	55.4 (1,998.0)	116.9 (2,000.0)	14.2 (1,661.0)	0.0		
TSZ	24.8 (1,909.9)	48.2 (1,995.2)	24.7 (1,909.9)	105.7 (2,000.0)	57.8 (1,998.5)	42.2 (1,989.7)	0.0	
GS	391.5 (2,000.0)	128.1 (2,000.0)	124.8 (2,000.0)	132.9 (2,000.0)	81.9 (1,999.9)	155.9 (2,000.0)	309.5 (2,000.0)	0.0
DGS	400.3 (2,000.0)	138.5 (2,000.0)	118.9 (2,000.0)	98.7 (2,000.0)	136.8 (2,000.0)	223.7 (2,000.0)	344.3 (2,000.0)	8.6 (1,313.4)

References

Aldrich, R.C. Detecting disturbances in a forest environment. *Photogrammetric Engineering and Remote Sensing,* 41, 1975. p. 39-48.

Beaubien, J. Visual interpretation of vegetation through digitally enhanced Landsat MSS images. *Remote Sensing Review,* 2, 1986. p. 111-143.

Horler, D.N.H. and F.J. Ahren. Forestry information content of Thematic Mapper data. *International Journal of Remote Sensing,* 7 (3), 1986. p. 405-428.

Jenson, J.R. *Digital Image Processing: A Remote Sensing Perspective.* Prentice-Hall, Englewood Cliffs, N.J., 1986.

Kauth, R.J. and G.S. Thomas. The tasselled cap: a graphic description of spectral-temporal development in machine processing of remotely sensed data. Laboratory for the Application of Remote Sensing, West Lafayette, Indiana, 1976. p. 41-51.

Kumar, R. and L.F. Silva. Separability of agricultural cover types by remote sensing in the visible and infrared wavelength regions. *IEEE*

Transactions in Geosciences Electronics, 15, 1977. p. 42-49.

Murai, S. and Y. Honda. Global change monitoring using the NOAA global vegetation index and geoinformation. *Asian-Pacific Remote Sensing Journal,* 4(1), 1991. p. 63-74.

Roy, P.S., B.K. Ranganath, P.G. Diwakar, T.P.S. Vohra, S.K. Bhan, I.J. Singh and V.C. Pandian. Tropical forest type mapping and monitoring using remote sensing data. *International Journal of Remote Sensing,* 12(11), 1991. p. 2,206-2,226.

Sabins, F.F. Jr. *Remote Sensing Principles and Interpretation,* second edition. Freeman, San Francisco, 1987. 449 p.

Schowengerdt, R.A. *Techniques for Image Processing and Classification in Remote Sensing.* Academic Press, New York, 1983.

Singh, A. Spectral separability of forest cover classes. *International Journal of Remote Sensing,* 8, 1987. p. 971-996.

Tateishi, R., K. Kajiwara and T. Odajima. Global landcover classification by phenological methods using NOAA GVI data. *Asian-Pacific Remote Sensing Journal,* 4(1), 1991. p. 41-50.

Tiwari, A.K., M. Kudrat and S.K. Bhan. Analysis of vegetation and soil associations in part of the western Himalaya. In *Mountain Resources Management and Remote Sensing,* Surya Publications, Dehra Dun, India, 1991.

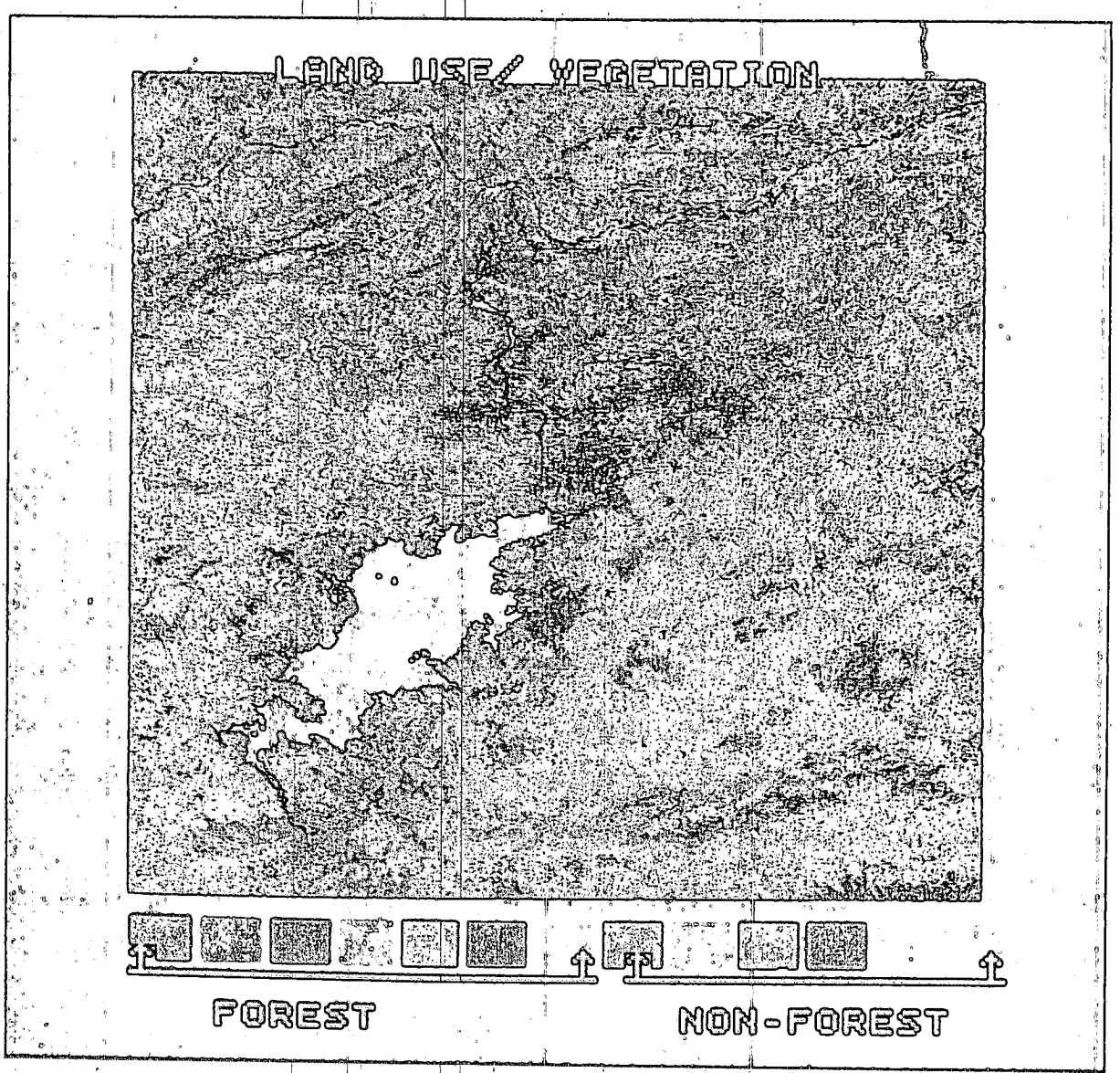

Figure 1. Unsupervised classification output. The colour sequence in the bottom of the image from left to right shows M1, M2, M3, SDF, ADF, TSH and TSZ classes and GS and DGS classes. Other colours represent nonforested land.

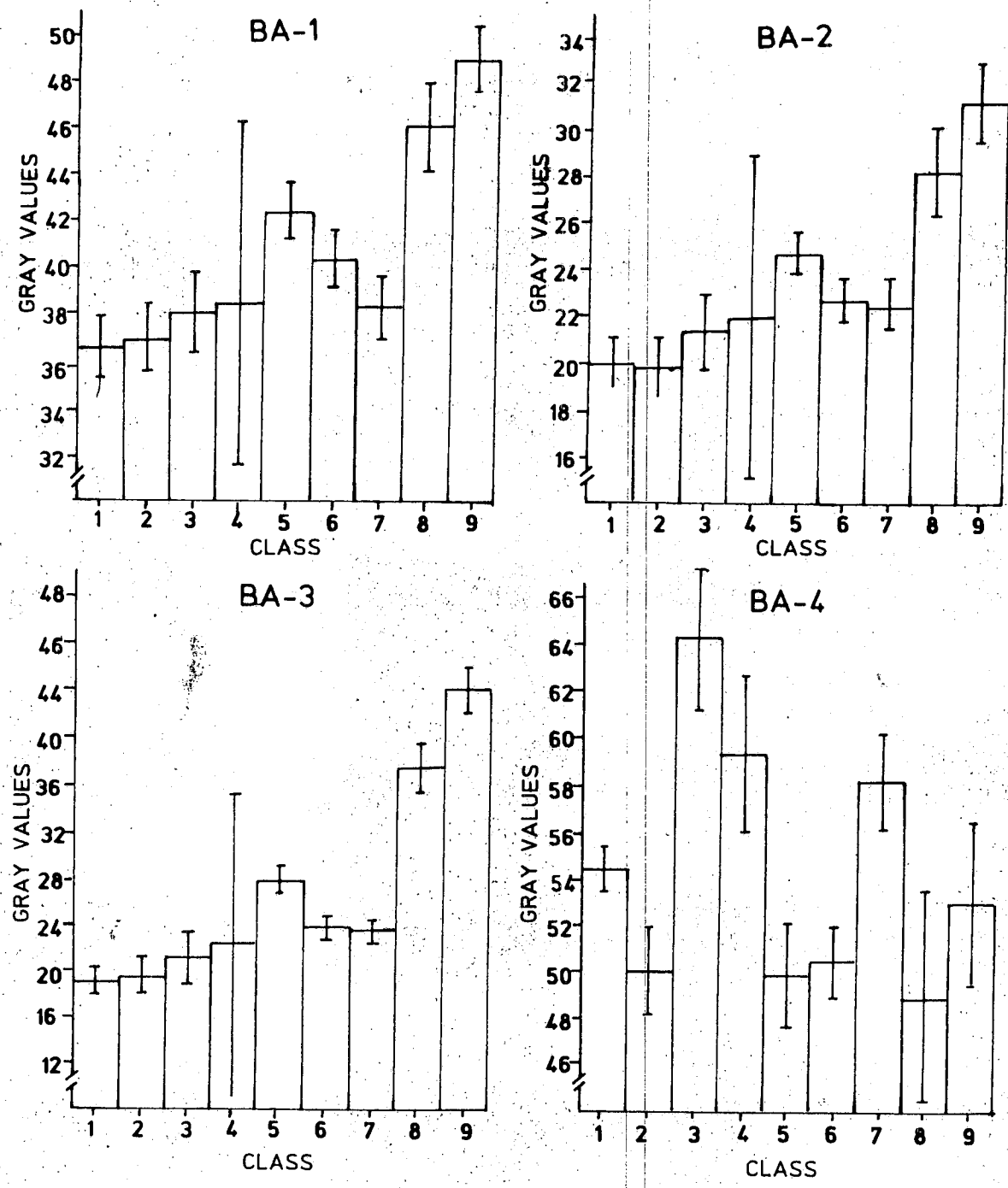

Figure 2. The spectral response of various vegetation classes in the IRS-1A LISS-I bands

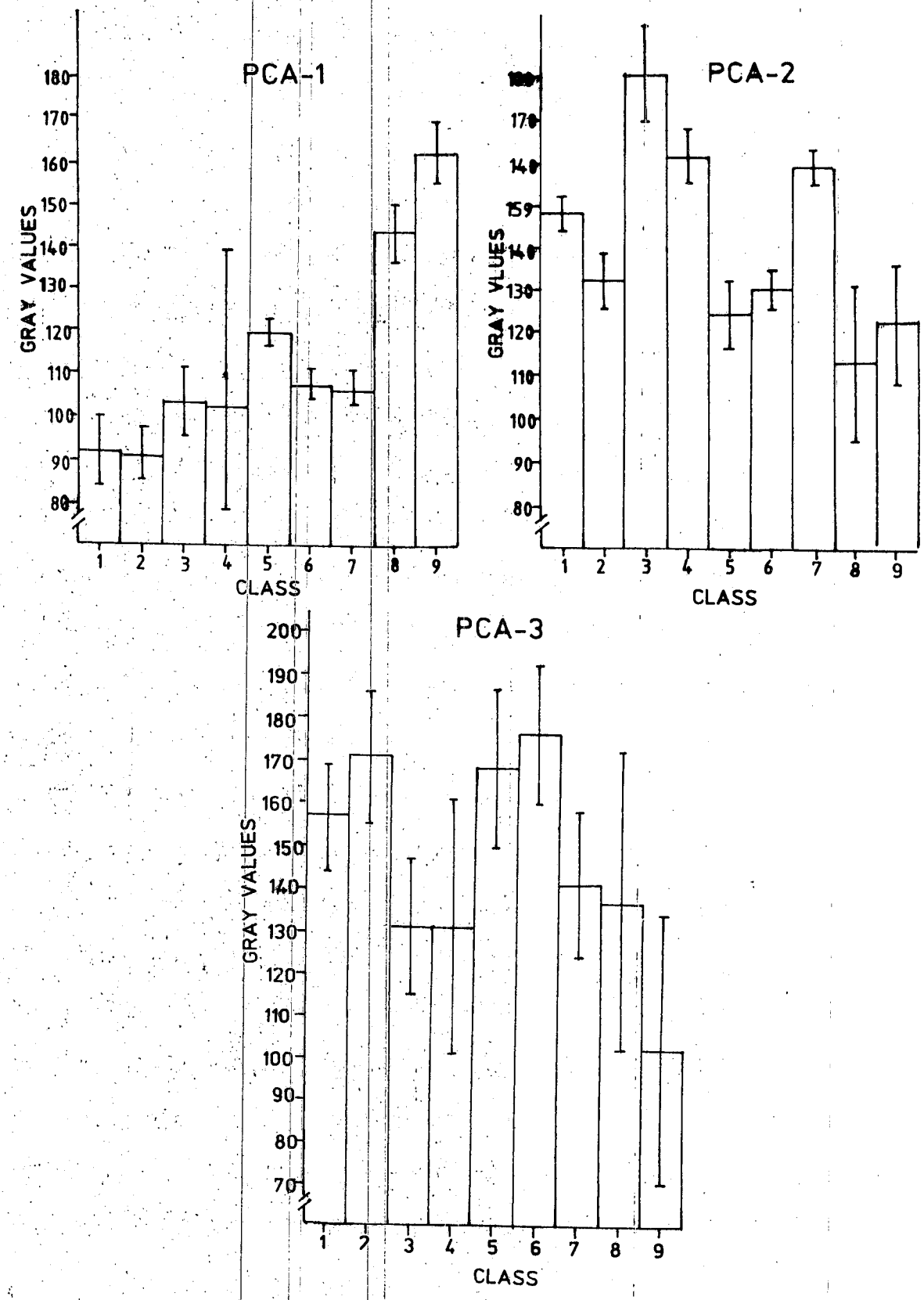

Figure 3. Mean growth values with ±SD for various vegetation classes in the PCA bands

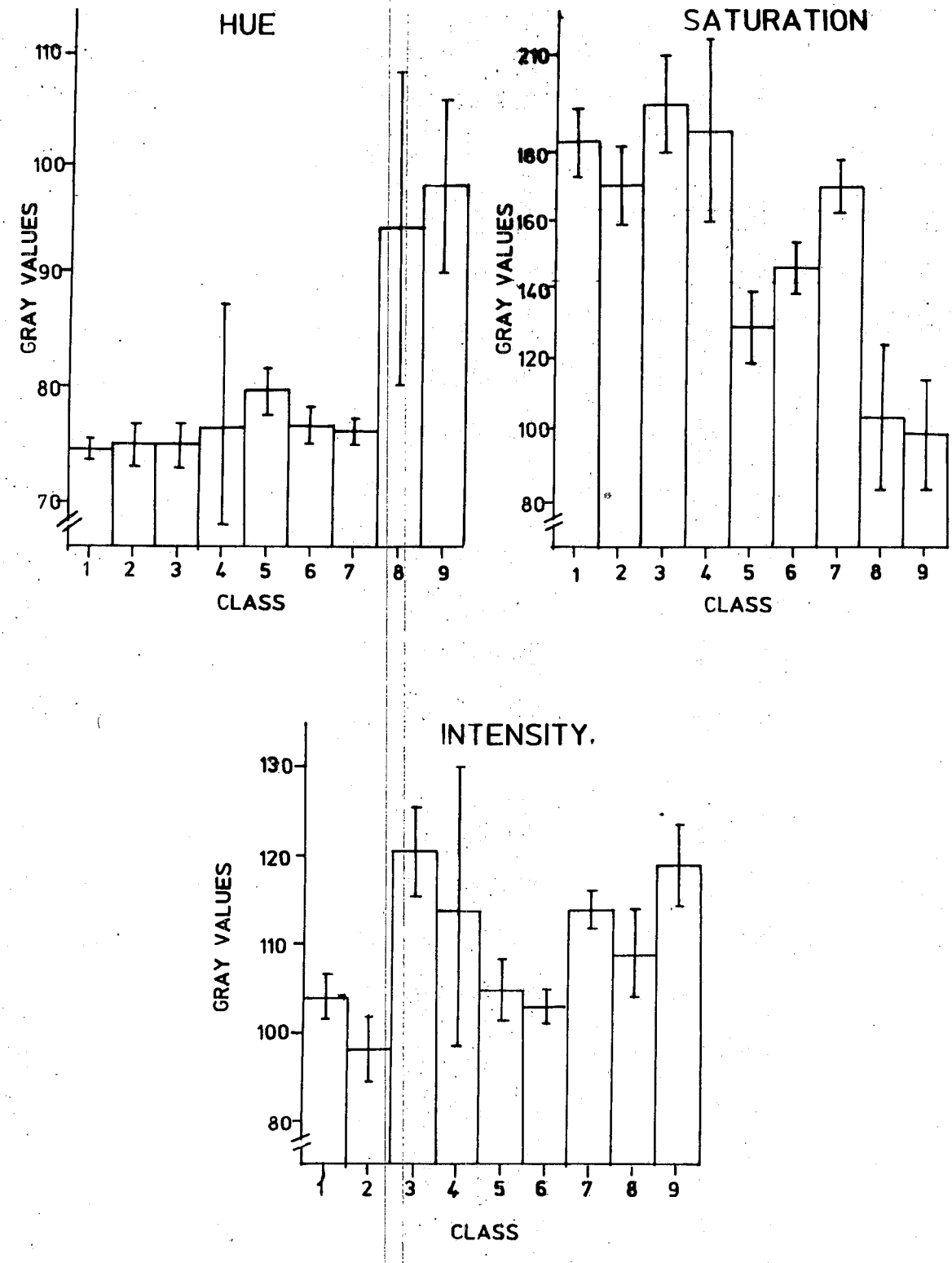

Figure 4. Mean DM value and ±SD for various vegetation classes in various HSI bands